DOI: 10.1002/ejic.200500999

One Dimensional 3d–4f Heterometallic Compounds: Synthesis, Structure and Magnetic Properties

Albert Figuerola,[a] Joan Ribas,[a] Xavier Solans,[b] Merce Font-Bardía,[b] Miguel Maestro,[c] and Carmen Diaz*[a]

Keywords: Lanthanides / Chromium / Cyanide / Magnetic properties

The reaction of $Ln(NO_3)_3 \cdot aq$ with $K_3[Fe(CN)_6]$ or $K_3[Co(CN)_6]$ and 2,2′:6′,2′′-terpyridine in water/methanol solution led to three one-dimensional complexes: *trans*-$[Ln(H_2O)_4(terpy)(\mu\text{-}CN)_2M(CN)_4]_n$ (Ln = La^{3+} or Sm^{3+}; M = Fe^{3+} or Co^{3+}). The structures of $[SmFe]_n$ (**1**), $[SmCo]_n$ (**2**) and $[LaFe]_n$ (**3**) have been solved; the complexes **1** and **2** crystallize in the monoclinic space $P2_1/c$ and are isomorphous, complex **3** crystallizes in the triclinic space $P\bar{1}$. No significant magnetic interaction was found between the samarium(III) and the iron(III) ions.

Introduction

The design of supramolecular architectures with novel spin-carrier topologies is of current interest in the field of molecular magnetism. A successful strategy leading to heteropolymetallic systems with extended structures consists in self-assembly processes involving anionic building blocks, which contain a paramagnetic ion, and assembling complex cations with potentially free coordination sites. Cyano-bridged bimetallic systems with interesting magnetic and photomagnetic properties have been characterized.[1] Most of these systems contain two different transition-metal ions. In contrast, the lanthanide cations have not been used as much as nodes for the construction of cyano-bridged heteropolymetallic coordination networks.[2] Thus, although the research on cyano-bridged complexes has mainly focused on transition-metal ions with polycyanometallates and 4f ions, several compounds with different dimensionality have been reported.[3–19] In most cases the magnetic properties of these complexes do not seem exciting, as the coupling between the lanthanide and transition metals is very weak because of the effective shielding of the 4f electrons by the outer-shell electrons.

Important magnetic properties were found in only a few cyano-bridged rare earth transition-metal complexes. Most of the 3d–4f complexes that show long-range magnetic ordering involved the Sm^{3+} ion.[3b,4b,5,13a,20] We are exploring a strategy to control the structure in the solid state that combines elements of design towards crystal engineering and the study of magnetic properties. We successfully applied this strategy in the preparation of new species starting from the mononuclear species $[M(CN)_6]^{3-}$ (M = Fe^{3+}, Cr^{3+} and Co^{3+}) as building blocks, $Ln(NO_3)_3 \cdot xH_2O$ and different blocking ligands; a) with M = Fe^{3+} or Co^{3+} and dimethylformamide (DMF) as blocking ligand, working with the same conditions, we reported a family of 25 dinuclear complexes of the formula $[Ln(DMF)_4(H_2O)_3(\mu\text{-}CN)M(CN)_5] \cdot nH_2O$ (with Ln = all lanthanide(III) ions except Pm and Lu) (Scheme 1, a).[4a] Structural studies of these families show that they are isomorphous; b) changes in the anionic building block modifies the structural types: using $[Cr(CN)_6]^{3-}$, $Gd(NO_3)_3 \cdot 6H_2O$, DMF and the same conditions of reaction, a one-dimensional *cis*-$[Cr(CN)_4(\mu\text{-}CN)_2Gd(H_2O)(DMF)_4]_n \cdot nH_2O$ was previously reported by the authors (Scheme 1, c).[4c] c) Changes in the terminal blocking ligand introduce new changes in the structural types: reactions involving Ln^{3+} and $[Co(CN)_6]^{3-}$, $[Fe(CN)_6]^{3-}$ or $[Cr(CN)_6]^{3-}$ ions using bpy as terminal ligand instead of DMF lead to one-dimensional complexes of formula *trans*-$[M(CN)_4(\mu\text{-}CN)_2Ln(H_2O)(bpy)]_n \cdot XnH_2O$ (bpy = 2,2′-bipyridine) form the late lanthanide ions (Scheme 1, b)[4e] and trinuclear complexes of the formula *trans*-$[M(CN)_4(\mu\text{-}CN)_2\{Ln(H_2O)_4(bpy)_2\}_2][M(CN)_6] \cdot 8H_2O$ from the early ones (Scheme 1, d); for the one-dimensional complexes, hydrogen bonds and π–π interactions give three-dimensional networks. This work is focused on the synthesis, structures, and magnetic properties of the new one-dimensional compounds with 2,2′:6′,2′′-terpyridine (terpy) (Scheme 1, e)

---

[a] Departament de Química Inorgànica, Universitat de Barcelona,
Martí i Franquès 1–11, 08028 Barcelona, Spain
E-mail: carme.diaz@qi.ub.es
[b] Departament de Cristallografia Mineralogia i Dipòsits Minerals, Universitat de Barcelona,
Martí I Franquès s/n, 08028 Barcelona, Spain
[c] Departamento de Química Fundamental, Universidade da Coruña
15071 A Coruña, Spain

Supporting information for this article is available on the WWW under http://www.eurjic.org or from the author.

acting as blocking ligand: *trans*-[$Sm(H_2O)_4(terpy)(\mu\text{-}CN)_2Fe(CN)_4]_n$ (**1**), *trans*-[$Sm(H_2O)_4(terpy)(\mu\text{-}CN)_2Co(CN)_4]_n$ (**2**) and *trans*-[$La(H_2O)_4(terpy)(\mu\text{-}CN)_2$ $Fe(CN)_4]_n$ (**3**).

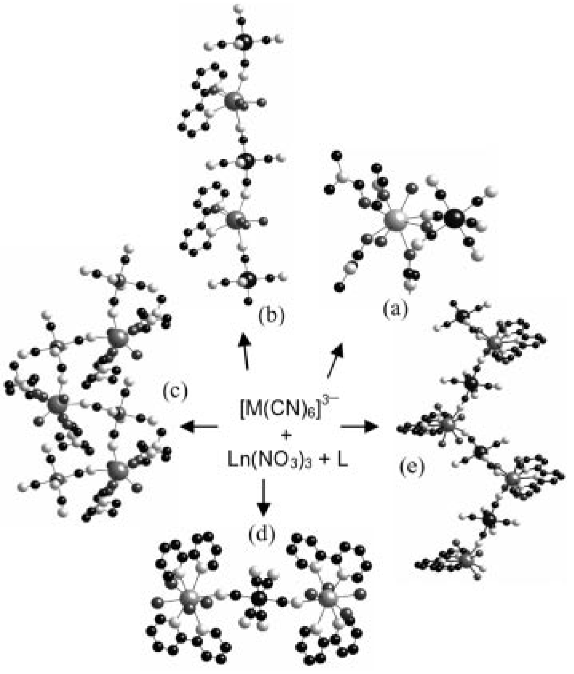

Scheme 1.

Results and Discussion

Description of the Structure of Complexes 1–3

Their crystallographic analysis revealed that complex **1** and **2** are isomorphous. Complexes **1** and **2** crystallize in the monoclinic system and complex **3** in the triclinic system. The structure of the three complexes consists of one-dimensional (1-D) chain polymer. An ORTEP view of [SmCo]$_n$ (**2**) and [LaFe]$_n$ (**3**) complexes with the atom-labeling scheme is given in Figure 1 and Figure 2, respectively. Selected bond lengths and angles for **1**–**3** are listed in Table 1. The coordination sphere around the Ln^{3+} ion comprises three nitrogen atoms of the 2,2′:6′,2′′-terpyridine ligand, four oxygen atoms of four water molecules, and two nitrogen atoms of the cyanide bridges, their coordination number is nine. Six cyanide ligands surround the M^{3+} (Fe, Co) ion in a distorted octahedral environment. In complex **3** the La–O and La–N distances are longer than the Sm–O and Sm–N of complexes **1** and **2** in accordance with the variation of the radius of the two-lanthanide ions. The lowest M–C distances correspond as expected to the $[Co(CN)_6]^{3-}$. In the three complexes, the chains show an alternation of [$Ln(H_2O)_4$(terpy)] and [$M(CN)_6$] (M^{3+} = Fe, Co) fragments linked by cyanide bridges in the *trans* geometry, a schematic view of the chain of [SmFe]$_n$ (**1**) and [LaFe]$_n$ (**2**) are shown in Figure 3. In the complexes **1** and **2** the distances M–Sm (M^{3+} = Co, Fe) are the same along the chain, but in complex **3** there are two different distances Fe1–La of 5.412 and Fe2–Ln of 5.446 Å. For complexes **1** and **2**, the angles Sm–M–Sm and M–Sm–M are different (176.48 and 102.32° for **1**, and 175.73 and 102.97° for **2**). For complex **3**, the angles values Fe1–La–Fe2, La–Fe1–La and La–Fe2–La are 103.69°, 179.97° and 179.98°, respectively. The chains are not in a linear configuration, the [LnMLn] trinuclear entities run along the chain in a zigzag path. An interesting feature of the conformation of the ligands around the Sm^{3+} and La^{3+} (complex **3**) ions is that they are chiral. As each Sm^{3+} (complexes **1** and **2**) is related to the neighboring one by a glide plane, there are two enantiomeric coordination spheres in an achiral chain. In complex **3**, each La^{3+} ion is related to the neighboring one by the inversion center at the Fe^{3+} ion that is bridging them, there are two enantiomeric coordination spheres in the achiral trinuclear unit. For complexes **1**–**3**, the supramolecular structures are created by hydrogen bonding. Shortest inter-contacts for complexes **1** and **2** (the hydrogen atoms of coordinated water molecules were not located) are listed in the Supporting Information, Table S1 (for details see the footnote on the first page of

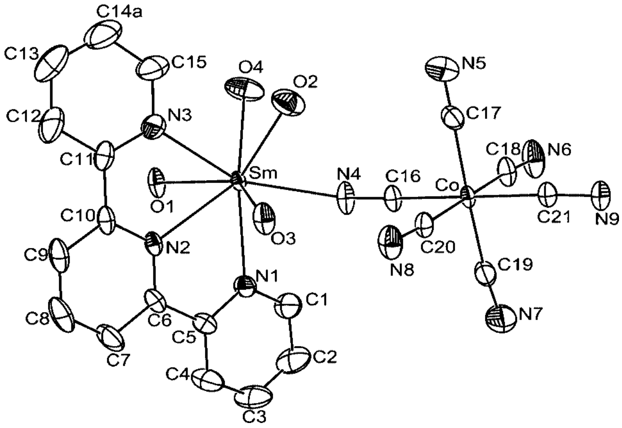

Figure 1. ORTEP view of complex *trans*-[SmCo]$_n$ (**2**) with atom labeling Scheme (ellipsoids draw at 50% probability level).

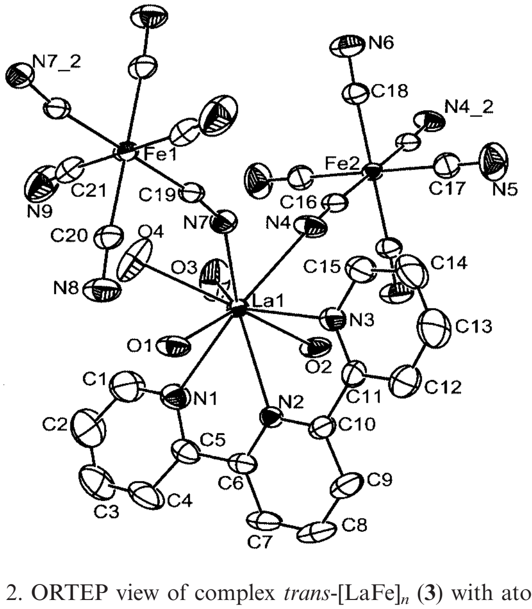

Figure 2. ORTEP view of complex *trans*-[LaFe]$_n$ (**3**) with atom labeling scheme (ellipsoids draw at 50% probability level).

Table 1. Selected bond lengths [Å] and angles [°] for **1**–**3**.

	$[SmFe]_n$ (**1**)	$[SmCo]_n$ (**2**)		$[LaFe]_n$ (**3**)
Sm–O(1)	2.460(3)	2.4660(16)	La(1)–O(1)	2.533(2)
Sm–O(2)	2.572(4)	2.558(2)	La(1)–O(2)	2.562(2)
Sm–O(3)	2.475(3)	2.4723(17)	La(1)–O(3)	2.623(2)
Sm–O(4)	2.503(4)	2.489(2)	La(1)–O(4)	2.561(3)
Sm–N(1)	2.592(3)	2.576(2)	La(1)–N(1)	2.666(3)
Sm–N(2)	2.654(4)	2.5667(18)	La(1)–N(2)	2.660(2)
Sm–N(3)	2.579(5)	2.582(2)	La(1)–N(3)	2.656(2)
Sm–N(4)	2.514(4)	2.497(2)	La(1)–N(4)	2.601(2)
Sm–N(9)	2.538(4)	2.5428(19)	La(1)–N(7)	2.609(2)
M–C(16)	1.909(5)	1.873(2)	Fe(1)–C(19)	1.926(3)
M–C(17)	1.941(5)	1.889(3)	Fe(1)–C(20)	1.947(3)
M–C(18)	1.954(5)	1.896(2)	Fe(1)–C(21)	1.937(3)
M–C(19)	1.943(6)	1.890(3)	Fe(2)–C(16)	1.926(3)
M–C(20)	1.953(5)	1.900(2)	Fe(2)–C(17)	1.930(3)
M–C(21)	1.940(5)	1.8837(19)	Fe(2)–C(18)	1.945(3)
N(4)–C(16)	1.142(6)	1.151(3)	N(7)–C(19)	1.144(4)
Sm–N(4)–C(16)	154.4(4)	154.4(2)	La(1)–N(4)–C(16)	152.2(2)
M–C(16)–N(4)	173.0(4)	172.5(2)	La(1)–N(7)–C(19)	150.4(2)
			Fe(2)–C(16)–N(4)	173.3(3)
			Fe(1)–C(19)–N(7)	171.4(3)

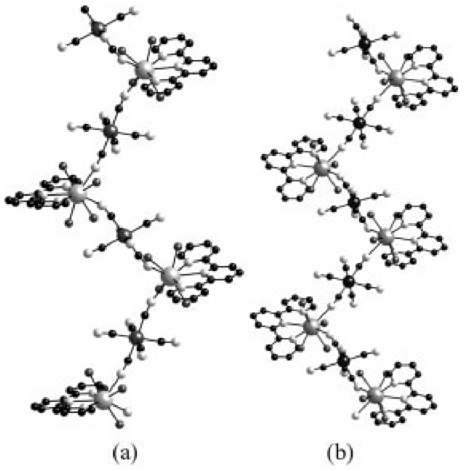
(a) (b)

Figure 3. Schematic representation of the chains of $[SmFe]_n$ (a) and $[LaFe]_n$ (b).

this article); for complex **3**, the distances and angles corresponding to the hydrogen bonds are listed in the Supporting Information, Table S2. Complexes **1** and **2** show the same pathway of hydrogen bonds, but different than complex **3**. In complexes **1** and **2** the chains are self-assembled through hydrogen bonds in two different pathways. The O1 and O4 atoms of two coordinated water molecules to the samarium(III) ion and the two nitrogen atoms, N5 and N8 of the $[M(CN)_6]$ entity, give an extensive 3D network. In Figure 4 the different ways and the atoms involved in the self-assembled structure for complex $[SmFe]_n$ (**1**), as example, are shown. In complex **3**, the O1, O2 and O3 oxygen atoms of the coordinated water molecules to the lanthanum(III) ion and three nitrogen atoms, N5, N6 and N8 of the $[Fe(CN)_6]$ entity, give an extensive 3D network. In Figure 5 the different ways and the atoms involved in the self-assembled structure for complex $[LaFe]_n$ (**3**) are shown. The π–π interactions between the terpy ligands of neighboring chains are

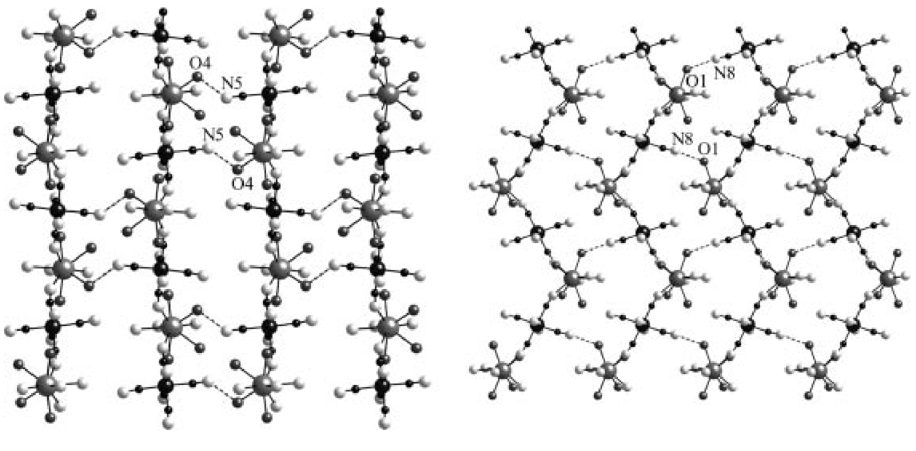

Figure 4. Schematic representation, for complex $[SmFe]_n$ (**1**), of different pathways in which the chains are self-assembled through hydrogen bonds. Complex **2** show similar self-assembly.

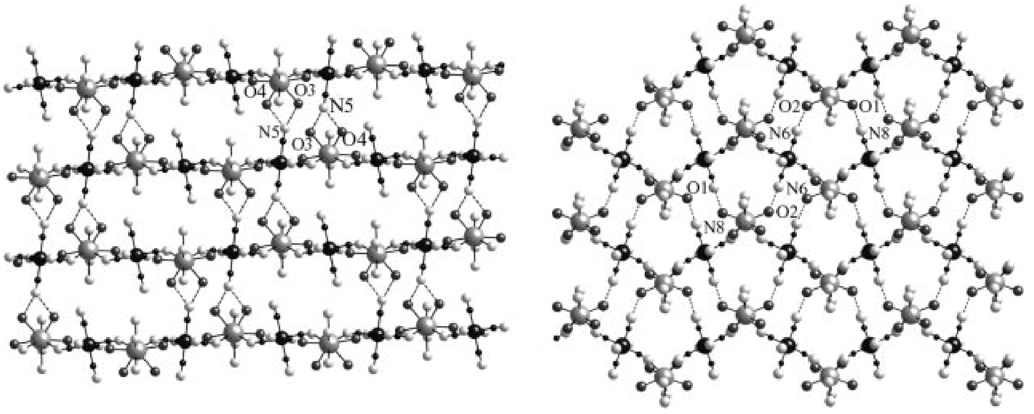

Figure 5. Schematic representation, for complex [LaFe]$_n$ (**3**), of different pathways in which the chains are self-assembled through hydrogen bonds.

very weak. Intermolecular stacking distances between centroids of the terpy rings are shown for complexes **1**–**3** in the Supporting Information, Table S3.

Magnetic Properties: Magnetic measurements were performed for the [SmFe]$_n$ (**1**), [SmCo]$_n$ (**2**) and [LaFe]$_n$ (**3**) complexes. The Sm^{3+} and the Fe^{3+} ions possess a first-order angular momentum, which prevents the use of a spin-only Hamiltonian for isotropic exchange. Not much is known about the nature of the exchange interaction of rare earth ions between themselves and with other magnetic groups, because the large orbital contribution of these ions makes a quantitative interpretation of the magnetic data of their complexes very complicated. The difficulty in having quantitative information on both these contributions has so far reduced the analysis of the magnetic properties of the anisotropic lanthanides mainly at a qualitative level, especially in molecular complexes. The most diffuse experimental approach to separate the different contributions of crystal field and exchange coupling to the magnetic properties in either heterometallic or lanthanide radical complexes involves the determination of magnetic properties of a corresponding complex where the second spin carrier is substituted by a diamagnetic analog, which gives rise to comparable ligand-field effects on the lanthanides.[21,4a,4b,4d,4e] Together with the [SmFe]$_n$ complex, we attempted to synthesize and characterize the homologous [SmCo]$_n$ and [LaFe]$_n$ complexes to use the typical empirical approach, mentioned above, to obtain insights into the nature of the [SmFe]$_n$ coupling. The approach consists of comparing its magnetic susceptibility data with the corresponding isostructural [SmCo]$_n$ compounds together with the magnetic properties of the [LaFe]$_n$ complex to take the anisotropy of the Fe^{3+} ion into account. The Co^{3+} and the La^{3+} ions are obviously diamagnetic, and the deviation of the magnetic susceptibility of the [SmCo]$_n$ and the [LaFe]$_n$ compounds with respect to the Curie law is due entirely to the thermal population of the Sm^{3+} Stark components and the anisotropy of Fe^{3+}, respectively. The comparison of the experimental magnetization at low temperature of the exchange-coupled system with that of the corresponding uncorrelated spin systems constitutes a further way to discriminate the sign of the coupling. Indeed if the M vs. H curve of the coupled system is running below the curve of the non-correlated system; an antiferromagnetic interaction within the molecular spin system is revealed, while the reverse would be true for a ferromagnetic situation.[22]

For most of the rare-earth compounds, the $\chi_M T$ value at room temperature is close to what is predicted in the free-ion approximation for the cases where only one level, $^{2S+1}L_j$, is thermally populated and second-order contributions are ignored.[23] For the complexes containing the Sm^{3+} ion, the magnetic susceptibility is affected by the thermally populated excited states because of the spin-orbit coupling. The [LaFe]$_n$ complex is not isostructural with the [SmFe]$_n$ and [SmCo]$_n$ ones, but taking into account that the structural features round the [Fe(CN)$_6$] entity are very similar in the three complexes, we can consider that the crystal field parameters around the Fe^{3+} ion are analogous. So we apply the approach in order to evaluate the presence or not of magnetic interaction between the Sm^{3+} and Fe^{3+} ions.

***trans*-[Sm(H$_2$O)$_4$(terpy)(μ-CN)$_2$Fe(CN)$_4$]$_n$, *trans*-[Sm(H$_2$O)$_4$(terpy)(μ-CN)$_2$Co(CN)$_4$]$_n$ and *trans*-[La(H$_2$O)$_4$(terpy)(μ-CN)$_2$Fe(CN)$_4$]$_n$:** The temperature dependence of the $\chi_M T$ for the three complexes is shown in Figure 6 (top). For the [SmCo]$_n$ complex, the $\chi_M T$ value at 300 K is approximately equal to 0.37 cm^3 mol^{-1} K. At room temperature, allowing for $\chi_M T$ = 0.05 cm^3 mol^{-1} K of Co^{3+} (l.s), from the TIP value for the Co^{3+} ion,[24] the $\chi_M T$ value corresponding to the Sm^{3+} is 0.32 cm^3 mol^{-1} K. At room temperature, the experimental $\chi_M T$ values found in the literature are around 0.32 cm^3 mol^{-1} K. These observed values are inconsistent with the theoretical value of 0.09 cm^3 mol^{-1} K expected for one Sm^{3+} ($^6H_{5/2}$) ion. This disagreement is ascribed to the presence of thermal populated excited states, as is well known for Sm^{3+} complexes. On lowering the temperature, the $\chi_M T$ value decreases monotonically to 0.05 cm^3 mol^{-1} K. For the [LaFe]$_n$ complex, the $\chi_M T$ value at 300 K is approximately equal to 0.80 cm^3 mol^{-1} K, while it decreases with temperature to 0.53 cm^3 mol^{-1} K. For the [SmFe]$_n$ complex, the $\chi_M T$ value at 300 K is approximately equal to 1.14 cm^3 mol^{-1} K, while it decreases with temperature to 0.63 cm^3 mol^{-1} K. The $\chi_M T$

value at room temperature fits nicely to the sum (1.12 $cm^3 mol^{-1} K$) of the measured values for the Sm^{3+} ion (0.32 $cm^3 mol^{-1} K$) in the $[SmCo]_n$ complex and for the Fe^{3+} ion (0.80 $cm^3 mol^{-1} K$) in the $[LaFe]_n$ complex. The $\Delta\chi_M T$ vs. T curve is practically superimposable with the $\chi_M T$ vs. T curve of the $[LaFe]_n$ complex along the whole range of temperatures indicating that no noticeable interaction is active. The experimental magnetization of $[SmFe]_n$ at 2 K (Figure 6, bottom) is superimposable with that of the uncorrelated spin system, corroborating that no exchange interaction is active.

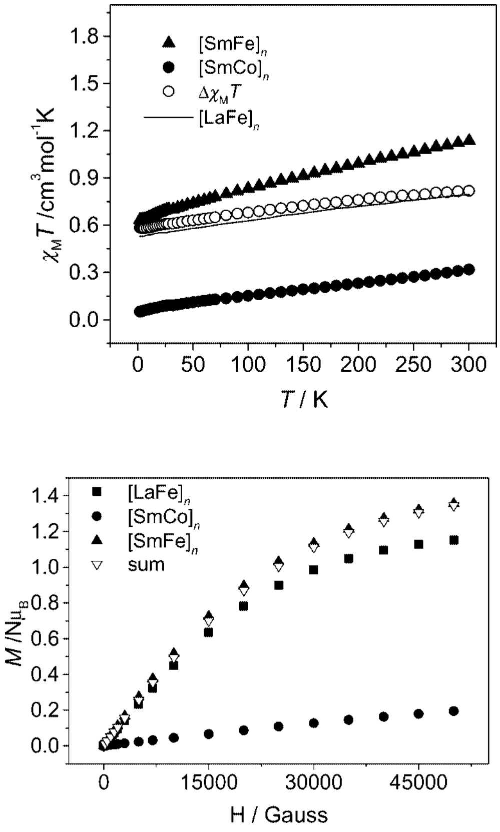

Figure 6. Top: thermal dependence at 0.1 T of $\chi_M^{[SmFe]_n}T$, $\chi_M^{[SmCo]_n}T$, $\chi_M^{[LaFe]_n}T$ and $\Delta\chi_M T = \chi_M^{[SmFe]_n}T - \chi_M^{[SmCo]_n}T$, the TIP value of the Co^{3+} ion has been considered (see text). Bottom: magnetization vs. H (2 K) of $M^{[SmFe]_n}$, $M^{[SmCo]_n}$, $M^{[LaFe]_n}$ and sum $M^{[LaFe]_n} + M^{[SmCo]_n}$.

Conclusions

Three one-dimensional $[SmFe]_n$, $[SmCo]_n$ and $[LaFe]_n$ complexes, have been structurally characterized and magnetically studied. Most of the 3d–4f complexes that show long-range magnetic ordering involved the Sm^{3+} ion. The replacement of Sm^{3+} ion by another lanthanide ion usually gives rise to isostructural compounds that lose all three-dimensional magnetic properties. Unfortunately the magnetic interaction between the Sm^{3+} and the Fe^{3+} ions in the $[SmFe]_n$ complex is negligible. Trying to make magneto-structural correlations has proved impossible until now due to the complexity of the 3d–4f magnetic interactions and to the few complexes reported in the literature with similar Ln–CN–Fe core.

Experimental Section

Materials: All starting materials were purchased from Aldrich and were used without further purification.

Physical Measurements: Magnetic measurements were carried out in the "Servei de Magnetoquímica (Universitat de Barcelona)" on polycrystalline samples (20 mg) with a Quantum Design SQUID MPMS-XL magnetometer working in the 2–300 K range. The magnetic field was 0.1 T. The field-dependent magnetization was measured in the applied magnetic field range 0–5 T. The diamagnetic corrections were evaluated from Pascal's constants.

Synthesis of *trans*-$[Sm(H_2O)_4(terpy)(\mu\text{-}CN)_2Fe(CN)_4]_n$(1), and *trans*-$[La(H_2O)_4(terpy)(\mu\text{-}CN)_2Fe(CN)_4]_n$ (3): The two $[Ln–Fe]_n$ complexes were obtained by adding a solution of $Ln(NO_3)_3\cdot nH_2O$ (0.2 mmol) in water (50 mL) to an equimolar solution of $K_3[Fe(CN)_6]$ in water (50 mL). To this mixture an ethanolic solution (20 mL) of 2,2′:6′,2′′-terpyridine (0.3 mmol) was added. The solution was left undisturbed, and well-formed crystals (orange for both complexes) were obtained after several days.

Synthesis of *trans*-$[Sm(H_2O)_4(terpy)(\mu\text{-}CN)_2Co(CN)_4]_n$ (2): The complex was obtained by the same procedure using $K_3[Co(CN)_6]$ instead of $K_3[Fe(CN)_6]$. Well-formed colourless crystals were obtained after several days.

Complex 1: Yield: 100 mg (75%). $C_{21}H_{19}FeN_9O_4Sm$ (667.65): calcd. C 40.70, N 16.84, H 4.19; found C 40.9, N 17.0, H 4.0.

Complex 2: Yield: 107 mg (80%). $C_{21}H_{19}CoN_9O_4Sm$ (670.73): calcd. C 41.44, N 17.15, H 4.04; found C 41.5, N 17.2, H 4.0.

Complex 3: Yields: 96 mg (73%). $C_{21}H_{18}FeLaN_9O_4$ (656.19): calcd. C 41.20, N 17.05, H 4.01; found C 41.1, N17.2, H 3.9.

Crystallographic Studies: Crystal data and refinement are summarized in Table 2. Prismatic crystals, (0.1 × 0.1 × 0.2 mm), (0.1 × 0.2 × 0.2 mm) and (0.1 × 0.3 × 0.3 mm) of complexes **1**, **2** and **3** were selected and mounted on a Enraf–Nonius CAD4 four-circle diffractometer for **1**, on a MAR 345 diffractometer with an image plate detector for **2**, and on a Bruker SMART-CCD area diffractometer for **3**. Unit-cell parameters were determined from automatic centering of 25 reflections ($12 < \theta < 21°$) for **1**, from 24410 reflections ($3 < \theta < 21°$) for **2**, and from 1271 frames of intensity data covering 0.3° in ω over a hemisphere of the reciprocal space by combination of three exposure sets, and refined by least-square method for **3**. Intensities were collected with graphite-monochromatized Mo-K_α radiation (λ = 0.71073 Å), using $\omega/2\theta$ for **1** and **3**, and φ scan-technique for **2**; 7269 reflections for **1**, 26881 for **2** and 8230 for **3** were measured in the range $2.43 \leq \theta \leq 29$, $2.45 \leq \theta \leq 31.55$, and $2.12 \leq \theta \leq 28.31$, respectively. For complex **2**, 7477 of which were non-equivalent by symmetry [$R_{int}(I)$ = 0.017]; 4330 reflections of **1**, 7126 reflections of **2**, and 5231 of **3** were assumed as observed applying the condition $I > 2\sigma(I)$. Lorentz polarization and absorption corrections were made.

The structures were solved by Patterson synthesis for **1** and by direct methods for **2** and **3**, using SHELXS computer program[25] and refined by full-matrix least-squares method with SHELX97 computer program,[25] using 7269 reflections for **1**, 7477 reflections for **2**, and 5231 for **3**. The function minimized was $\Sigma w||F_o|^2 - |F_c|^2|^2$, where $w = [\sigma^2(I) + (0.0345P)^2]^{-1}$ for **1**, $w = [\sigma^2(I) + (0.0274P)^2 + 1.8065P]^{-1}$ for **2**, and $w = [\sigma^2(I) + (0.0297P)^2 + 0.8875P]^{-1}$ for **3**,

Table 2. Crystal parameters for **1**, **2** and **3**.

	$[SmFe]_n$ (**1**)	$[SmCo]_n$ (**2**)	$[LaFe]_n$ (**3**)
Empirical formula	$C_{21}H_{19}FeN_9O_4Sm$	$C_{21}H_{19}CoN_9O_4Sm$	$C_{21}H_{19}FeLaN_9O_4$
Formula mass	667.65	670.73	656.21
Crystal system	monoclinic	monoclinic	triclinic
Space group	$P2_1/c$	$P2_1/c$	$P\bar{1}$
Z	4	4	2
a [Å]	9.710(2)	9.625(1)	9.0673(7)
b [Å]	16.745(5)	16.656(1)	9.7385(7)
c [Å]	15.709(9)	15.706(1)	14.8550(11)
α [°]	90	90	84.9580(1)
β [°]	98.98(3)	99.28(1)	87.5980(10)
γ [°]	90	90	82.5540(10)
V [Å^3]	2522.9(17)	2484.9(3)	1295.01(17)
Radiation (Mo-K_α) [Å]	0.71069	0.71073	0.71073
$\rho_{calcd.}$ [g/cm^3]	1.758	1.793	1.683
$\mu_{calcd.}$ [mm^{-1}]	2.925	3.054	2.232
T [K]	293(2)	293(2)	298(2)
F[000]	1312	1316	643
Θ range for data	2.43–29.97°	2.45–31.55°	2.12–28.31°
Total reflections	7269	26881	8230
Independent reflections (R_{int})	7269 (0.0367)	7477 (0.0177)	5231 (0.0169)
Θ_{max} [%]	95.9	90.1	91.0
Parameters refined, restraints	313.0	353.0	328.8
Final R indices[a] [$I > 2\sigma(I)$]	$R_1 = 0.0341$	$R_1 = 0.0238$	$R_1 = 0.0256$
Final wR_2 indices[a]	$wR_2 = 0.0706$	$wR_2 = 0.0692$	$wR_2 = 0.0608$
Final R (for all data)[a]	$R_1 = 0.0896$	$R_1 = 0.0256$	$R_1 = 0.0312$
Final wR_2 (for all data)[a]	$wR_2 = 0.0830$	$wR_2 = 0.0701$	$wR_2 = 0.0632$
Goodness-of-fit on F^2	0.897	1.307	1.012

[a] $R_1 = \Sigma||F_o| - |F_c||$ and $wR_2 = \{\Sigma[w(F_o^2 - F_c^2)]/\Sigma[w(F_o^2)^2]\}^{1/2}$.

and $P = (|F_o|^2 + 2|F_c|^2)/3$, f, f' and f'' were taken from International Tables of X-ray Crystallography.[26] For **1** all non-water hydrogen atoms were computed and refined, using a riding model. For complex **2**, 7 hydrogen atoms were located from a difference synthesis and 4 hydrogen atoms were computed and refined using a riding model. For complex **3**, 4 hydrogen atoms were located from a difference synthesis and refined using a riding model. For all complexes, the isotropic temperature factor for H atoms was equal to 1.2 times the equivalent temperature factor of the atom, which is linked. For complex **1**, the final R (on F) factor was 0.034, wR (on $|F|^2$) = 0.070 and goodness of fit = 0.897 for all observed reflections; for complex **2**, the final R (on F) factor was 0.0238, wR (on $|F|^2$) = 0.0692 and goodness of fit = 1.307 for all observed reflections; and for complex **3**, the final R (on F) factor was 0.0256, wR (on $|F|^2$) = 0.0608 and goodness of fit = 1.012 for all observed reflections. For complex **1**, the number of refined parameters was 313. Max. shift/esd. = 0.00, Mean shift/esd. = 0.00. Max. and min. peaks in final difference synthesis was 0.802 and –0.811 e·Å^{-3}, respectively. For complex **2**, the number of refined parameters was 353. Max. shift/esd. = 0.00, Mean shift/esd. = 0.00. Max. and min. peaks in final difference synthesis was 0.583 and –0.518 e·Å^{-3}, respectively. For complex **3**, the number of refined parameters was 328, 8 restrictions were applied. Max. shift/esd. = 0.01, Mean shift/esd. = 0.00. Max. and min. peaks in final difference synthesis was 0.590 and –0.79 e·Å^{-3}, respectively.

CCDC-289051 (for **1**), -289050 (for **2**) and -289049 (for **3**) contain the supplementary crystallographic data for this paper. These data can be obtained free of charge from Cambridge Crystallographic Data Center via www.ccdc.cam.ac.uk/data_request/cif.

Supporting Information (see also the footnote on the first page of this article): Additional Tables with hydrogen bonds and π–π interactions.

Acknowledgments

This work was financially supported by the Spanish Government (Grant BQU2003–00539).

---

[1] a) V. Marvaud, C. Decroix, A. Sculler, C. Guyard-Duhayon, J. Vaissermann, F. Gonnet, M. Verdaguer, *Chem. Eur. J.* **2003**, *9*, 1677 an references therein; b) M. Ohba, H. Õkawa, *Coord. Chem. Rev.* **2000**, *198*, 313; c) M. Verdaguer, A. Bleuzen, V. Marvaud, J. Vaissermann, M. Seuleiman, C. Desplanches, A. Scuiller, C. Train, R. Garde, G. Gelly, C. Lomenech, I. Rosenman, P. Veillet, C. Cartier, F. Villain, *Coord. Chem. Rev.* **1999**, *190–192*, 1023.

[2] a) C. Benelli, D. Gatteschi, *Chem. Rev.* **2002**, *102*, 2369; b) G.-F. de Sá, O. P. Malta, C. de Mello Donegá, A. M. Simas, R. L. Longo, P. A. Santacruz, E. F. da Silva Jr, *Coord. Chem. Rev.* **2000**, *196*, 165.

[3] a) F. Hulliger, M. Landolt, H. Vetsch, *J. Solid State Chem.* **1976**, *18*, 307; b) F. Hulliger, M. Landolt, H. Vetsch, *J. Solid State Chem.* **1976**, *18*, 283.

[4] a) A. Figuerola, C. Diaz, J. Ribas, V. Tangoulis, J. Granell, F. Lloret, J. Mahía, M. Maestro, *Inorg. Chem.* **2003**, *42*, 641; b) A. Figuerola, C. Diaz, J. Ribas, V. Tangoulis, C. Sangregorio, D. Gatteschi, M. Maestro, J. Mahía, *Inorg. Chem.* **2003**, *42*, 5274; c) A. Figuerola, C. Diaz, M. S. El Fallah, J. Ribas, M. Maestro, J. Mahía, *Chem. Commun.* **2001**, 1204; d) A. Figuerola, J. Ribas, M. Llunell, D. Casanova, M. Maestro, S. Alvarez, C. Diaz, *Inorg. Chem.* **2005**, *44*, 6939; e) A. Figuerola, J. Ribas, D. Casanovas, M. Maestro, S. Alvarez, C. Diaz, *Inorg. Chem.* **2005**, *44*, 6949.

[5] H. Z. Kou, S. Gao, X. Jin, *Inorg. Chem.* **2001**, *40*, 6295.

[6] a) B. Q. Ma, S. Gao, G. Su, G. X. Xu, *Angew. Chem. Int. Ed.* **2001**, *40*, 434; b) R. Gheorghe, M. Andruh, J. P. Costes, B. Donnadieu, *Chem. Commun.* **2003**, 2778.

[7] D. W. Knoeppel, J. Liu, E. A. Meyers, S. G. Shore, *Inorg. Chem.* **1998**, *37*, 4828.

[8] B. Du, E. Ding, E. A. Meyers, S. G. Shore, *Inorg. Chem.* **2001**, *40*, 3637.

[9] B. Yan, H. D. Wang, Z. D. Chen, *Polyhedron* **2001**, *20*, 591.

[10] B. Yan, Z. Chen, S. Wang, S. Gao, *Chem. Lett.* **2001**, 350.

[11] S. Tanase, M. Andruh, A. Müller, M. Schmidtmann, C. Mathonière, G. Rombaut, *Chem. Commun.* **2001**, 1084.

[12] H. Z. Kou, S. Gao, C. H. Li, D. Z. Liao, B. C. Zhou, R. J. Wang, Y. Li, *Inorg. Chem.* **2002**, *41*, 4756.

[13] a) B. Yan, Z. Chen, *Helvetica Chim. Acta* **2001**, 817; b) B. Yan, Z. Chen, *Trans. Met., Chem.* **2001**, *26*, 287.

[14] S. Liu, E. A. Meyers, S. G. Shore, *Angw. Chem. Int. Ed.* **2002**, *41*, 3609.

[15] J. A. Kautz, D. F. Mullica, B. P. Cunningham, R. A. Combs, J. M. Farmer, *J. Mol. Struct.* **2000**, *523*, 175.

[16] H. Z. Kou, G. M. Yang, D. Z. Liao, P. Cheng, Z. H. Jiang, S. P. Yan, X. Y. Huang, G. L. Wang, *J. Chem. Crystallogr.* **1998**, *28*, 303.

[17] D. F. Mullica, J. M. Farmer, B. P. Cunningham, J. A. Kautz, *J. Coord. Chem.* **2000**, *49*, 239.

[18] a) B. Yan, Z. Chen, *Chem. Lett.* **2000**, *11*, 1244; b) Q. Yue, J. Yang, G. H. Li, W. Xu, J. S. Chen, S. N. Wang, *Inorg. Chem.* **2005**, *44*, 5241.

[19] a) T. Yi, S. Gao, X. W. Chen, C. H. Yan, B. G. Li, *Acta Crystallogr., Sect. C* **1998**, *54*, 41; b) H. Z. Kou, S. Gao, B. W. Sun, *J. Chem. Mater.* **2001**, *13*, 1431.

[20] H. L. Sun, H. Shi, F. Zhao, L. Qi, S. Gao, *Chem. Commun.* **2005**, 4339.

[21] a) J. P. Costes, F. Dahan, A. Dupuis, J. P. Laurent, *Chem. Eur. J.* **1998**, *4*, 1616; b) A. Caneschi, A. Dei, D. Gatteschi, S. Poussereau, L. Sorace, *Dalton Trans.* **2004**, 1048 and references there in.

[22] J. P. Sutter, M. L. Khan, O. Khan, *Adv. Mater.* **1999**, *11*, 863.

[23] O. Kahn, *Molecular Magnetism*, VCH: Weinheim, **1993**.

[24] a) B. N. Figgis, J. Lewis, *Prog. Inorg. Chem.* **1964**, *6*, 72; b) B.N. Figgis, *Compreh. Coord. Chem.* (Eds.: G. Wilkinson, R. D. Gillard, J. A. McClaverty), vol. 1, Theory and Background, Pergamon, Oxford **1987**, 273.

[25] G. M. Sheldrick, **1997**, *A computer program for determination of crystal structure*, University of Göttingen, Germany.

[26] International Tables of X-ray Crystallography, **1974**, Kynoch Press, vol. IV, pp. 99–100 and 149.

Received: November 9, 2005